Journal of Alloys and Compounds 509 (2011) 3667–3671

Contents lists available at ScienceDirect

Journal of Alloys and Compounds

journal homepage: www.elsevier.com/locate/jallcom

A study on crystallization, optical and electrical properties of the advanced ZITO thin films using co-sputtering system

K.J. Chen[a], F.Y. Hung[b,*], S.J. Chang[a], S.P. Chang[a], Y.C. Mai[c], Z.S. Hu[c]

[a] Institute of Microelectronics & Department of Electrical Engineering, Center for Micro/Nano Science and Technology, National Cheng Kung University, Tainan 701, Taiwan
[b] Institute of Nanotechnology and Microsystems Engineering, Center for Micro/Nano Science and Technology, National Cheng Kung University, Tainan 701, Taiwan
[c] Institute of Electro-Optical Science and Engineering, Center for Micro/Nano Science and Technology, National Cheng Kung University, Tainan 701, Taiwan

ARTICLE INFO

Article history:
Received 12 September 2010
Received in revised form
18 December 2010
Accepted 21 December 2010
Available online 29 December 2010

Keywords:
ZnO
ITO
Co-sputtering
Crystallization
Photoluminescence

ABSTRACT

Multi-functions (conductor, semiconductor and insulator) ZnInSnO (ZITO) transparent oxide thin films have been obtained by a co-sputtering system using ITO target and ZnO target with oxygen gas contents (0–8%). The ZITO film containing a small ITO content had the lowest resistivity (good electron mobility) and higher optical transmittance. In addition, the influences of thermal treatments (post-annealing and substrate temperature) on electrical properties and optical transmittance of ZITO films were studied. Photoluminescence (PL) of the ZITO film confirmed the contribution of ITO content and oxygen gas content on the photo-emission. The ZITO film with zinc atomic concentration of 58 at.% was a good candidate for TCO material ($3.08 \times 10^{-4}\ \Omega$ cm). Under the substrate temperature of 100 °C or post-annealing temperature of 200 °C, the properties of ZITO film could be improved.

© 2010 Elsevier B.V. All rights reserved.

1. Introduction

ZnO-based transparent conductive oxide (TCO) film has been received great attention due to its potential applications in transparency electrodes [1,2] and various optoelectronic devices [3–6]. To achieve better efficiency, various multi-compound TCO films were fabricated and further applied in optoelectronic device. Minami [7] used low-resistivity ZnO–In_2O_3 thin film to substitute for indium tin oxide (ITO) transparent electrode. Heo et al. [8] not only grew the Zn–In–Sn–O film (not co-sputtering method) at the substrate temperature of 250 °C, but also applied in the organic light-emitting diodes (OLEDs). The Zn–In–Sn–O film was further used as a transparent anode in fabrication of the flexible OLEDs [9]. In addition, amorphous semiconductor Zn–In–Sn–O materials have been also employed as the active layers of thin film transistors (TFTs) due to its high mobility (>10 cm^2/V s) and reasonable $I_{on/off}$ ratio (>10^6) [10,11].

The Zn–In–Sn–O (ZITO) films may have a potential application in different optoelectronic devices (photodetector, piezoelectric devices or gas sensor, etc.). Therefore, the variations in the ratios of ZnO to ITO and thermal effects (substrate and post-annealing temperatures) for the ZITO characteristics were worth to investigate. In addition, the luminescent quality mainly affected the photodetector performance, however the characteristics of photoluminescence (PL) for Zn–In–Sn–O (ZITO) film has never been reported.

Judging from the above, the multi-compound ZITO films (have conductive and semiconducting properties) were synthesized by co-sputtering system in present work, while the influences of the substrate temperatures (30–200 °C) and post-annealing temperatures (30–400 °C for 30 min) on electrical and optical properties of conductive ZITO film were also investigated. Notably, the ZITO films would be measured by photoluminescence (PL) to analyze the effects of ITO content and oxygen gas content on the emission characteristics.

2. Experimental procedures

ZITO films were co-deposited onto the glass substrate using an ITO target and a ZnO target (ULVAC, Model ACS-4000-C3). The initial pressure of deposition chamber was 2.3×10^{-5} Pa and the depositing pressure was kept at 1.9×10^{-1} Pa. The RF power supplied to the ZnO target was fixed at 80 W while the DC power supplied to ITO target was varied from 0 to 80 W, respectively. Contrarily, the ITO target was fixed at 80 W and then ZnO target was varied from 10 to 40 W. As a result, the ZITO films were referred to the ratio of zinc atomic concentration to the total atomic concentration of zinc and indium [Zn/(Zn + In) at.%]. In addition, the different functions (conductor and semiconductor) of ZITO films were obtained by adjusting the substrate temperature (30–200 °C) and oxygen partial pressure [O_2/(O_2 + Ar) = 0–8%] during the deposited process. To understand the contributions of post-annealing on conductivity and transmittance, the ZITO films were

* Corresponding author. Tel.: +886 6 2757575x31395; fax: +886 6 2745885.
E-mail address: fyhung@mail.mse.ncku.edu.tw (F.Y. Hung).

0925-8388/$ – see front matter © 2010 Elsevier B.V. All rights reserved.
doi:10.1016/j.jallcom.2010.12.155

also treated at different post-annealing temperatures (30–400 °C) for 30 min in vacuum.

The detailed compositions of all ZITO films were checked using an attached energy dispersive X-ray (EDX) spectroscope of a scanning electron microscope (SEM). The crystalline structure of ZITO films was examined by multipurpose X-ray thin film diffraction (XRD). In addition, the optical transmittance and electrical properties were measured by an UV–vis spectroscopy and the Hall measurement system, respectively. Finally, photoluminescence (PL) was used to analyze the optical quality by 325 nm UV light from a He–Cd laser at room temperature.

3. Results and discussion

3.1. Structural characteristics of ZITO films

Fig. 1 shows the X-ray diffraction patterns of ZITO films deposited at room temperature as a function of various zinc atomic concentration ratios [Zn/(Zn + In) at.%]. For pure ITO film, the polycrystalline structure with an obvious diffraction peak of (2 2 2) was obtained [12]. After a small amount of Zn [Zn/(Zn + In) = 5 at.%] was doped, the intensity of the major diffraction peaks decreased which indicating that the crystallization of ZITO film deteriorated. With increasing the Zn concentration at the atomic ratios varying from 5% to 21%, the ZITO films were still dominated by ITO polycrystalline structure. The intensity of (2 2 2) peak reached a maximum value at the atomic ratio of 17% and then decreased. Notably, the In_2O_3 phase was found at the Zn atomic concentration ratio reached 32%. Following, the polycrystalline structure was transformed into an amorphous-like structure at the Zn atomic concentration ratios varying from 58% to 69%. In fact, the crystallization of this ZITO film (69%) was dominated by $Zn_2In_2O_5$ phase and In_2O_3 phase (Fig. 1(c)). When the Zn atomic concentration was less than 69%, the crystallized effect of the In_2O_3 phases was quite obvious. This amorphous-like structure was similar to the data of previous literature [13] that may be applied in transistors. At the Zn atomic concentration ratio increased up to 76%, not only the $Zn_2In_2O_5$ phase existed, but also the related diffraction peak of ZnO appeared and dominated the ZITO film.

3.2. The effects of Zn atomic concentration

The resistivity, electron mobility and optical transmittance in visible region (390–800 nm) of ZITO films are shown in Fig. 2. These films were deposited at room temperature under a pure argon atmosphere (flow rate of 14 sccm). For pure ITO film, the film resistivity and electron mobility was $3.51 \times 10^{-4}\ \Omega$ cm and 9.67 cm^2/V s, respectively. With increasing the zinc atomic concentration ratio, the lowest resistivity of ZITO film ($1.62 \times 10^{-4}\ \Omega$ cm) was achieved at the Zn atomic concentration ratio of 32%. The main reason is that the Zn^{2+} ions not only substituted for In^{3+} ions sites, but also formed the oxygen vacancies resulted in the decrement of resistivity under the polycrystalline ITO structure region (0–32%) [14].

As the Zn atomic concentration ratio increased up 32%, the resistivity of ZITO films was gradually increased and the electron mobility decreased. These results were indicated that the existence of excess ZnO impurities not only decreased the film resistivity, but also promoted the decrement of electron mobility [15,16]. In addition, regardless of the Zn contents, the average transmittance in visible region (390–800 nm) of pure ITO film and all ZITO films possessed an excellent transparency (over 87%). To consider the cost (ITO content), ZITO film with a Zn atomic concentration ratio of 58% not only had a low resistivity ($3.08 \times 10^{-4}\ \Omega$ cm), fastest electron mobility (13.9 cm^2/V s), but also possessed an excellent optical transmittance that can be as good candidate for TCO electrode. According to XRD and electrical properties results, to adjust the oxygen content during the deposited process, the characteristics of ZITO films with a Zn atomic concentration ratio of 69–89% could be transformed from conductor to semiconductor that be suitable for active layer of thin film transistors (TFTs) and photodetector, respectively.

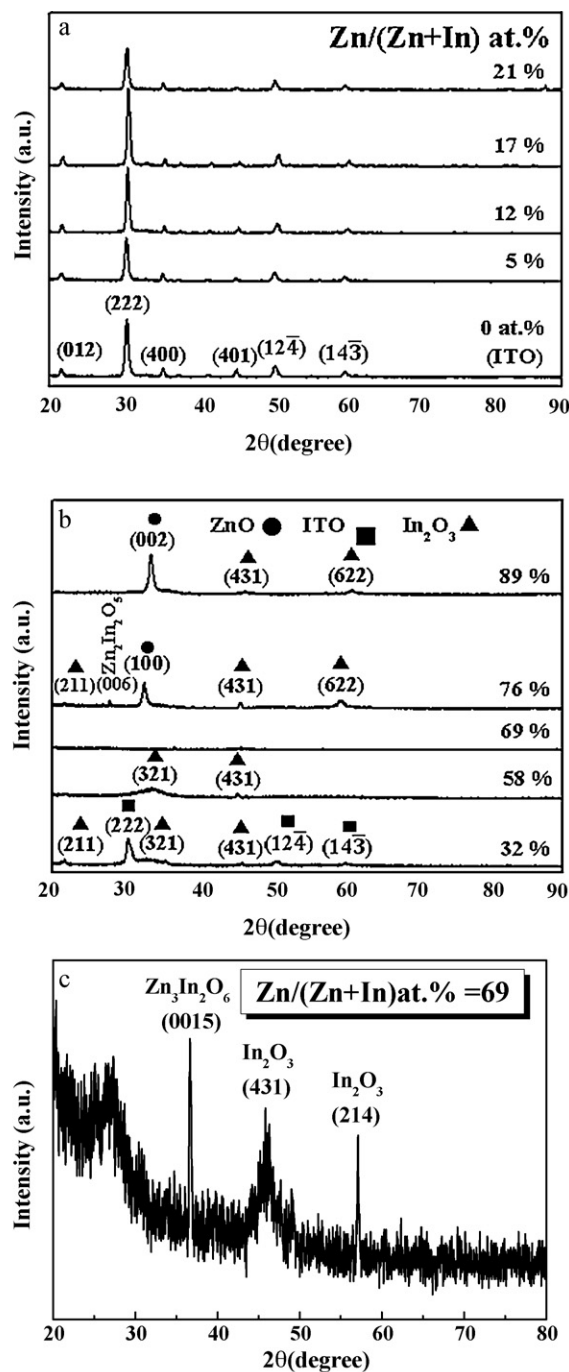

Fig. 1. X-ray diffraction patterns of ZITO films deposited with various zinc atomic concentration ratios. (a) 0–21 at.%, (b) 32–89 at.% and (c) the magnified pattern of 69 at.% film.

3.3. ZITO electrode (Zn atomic concentration ratio of 58%)

To understand the effects of substrate temperature and further apply in optoelectronic devices of flexible substrate, the ZITO film was deposited under the different substrate temperatures (30–200 °C). Fig. 3 shows the resistivity, electron mobility and optical transmittance of the ZITO film as a function of different substrate temperatures. With increasing the substrate temperature, the resistivity of ZITO film achieved a minimum value of

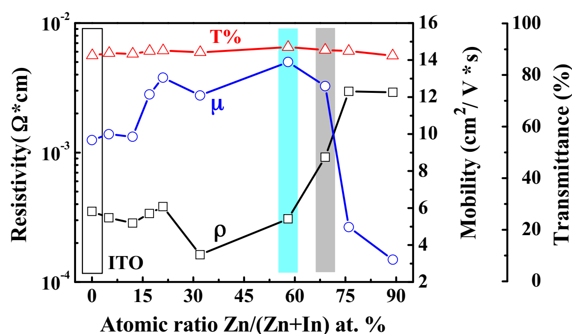

Fig. 2. Resistivity, electron mobility and optical transmittance as functions of zinc contents for ZITO films.

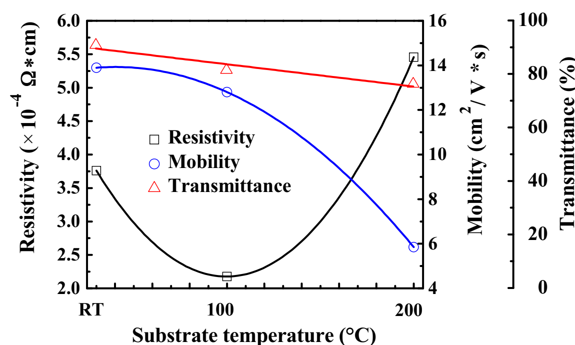

Fig. 3. Resistivity, electron mobility and optical transmittance of ZITO electrode deposited at different substrate temperatures.

$2.18 \times 10^{-4}\,\Omega\,$cm at substrate temperature of 100 °C and then increased. The decrement of resistivity was associated with the improvement of the crystallization quality and more formation of oxygen vacancies [17,18]. Contrarily, the resistivity increased as the substrate temperature more than 100 °C that attributed to the formation of oxygen vacancies were suppressed due to the oxygen atoms were prone to react with zinc atoms [8,19]. In addition, the electron mobility and average transmittance in visible range of ZITO film decreased when the substrate temperature increased which associated with the growth of grains [17,20,21].

The post-annealing is an important role for transparent conductive oxide thin film that not only improved the crystalline quality and electrical properties, but also enhanced the performance of optoelectronic devices [22,23]. Therefore, the resistivity and optical transmittance of ZITO electrodes annealed at different temperatures under vacuum as shown in Fig. 4. At lower annealing temperature (≤200 °C), the film resistivity decreased with the

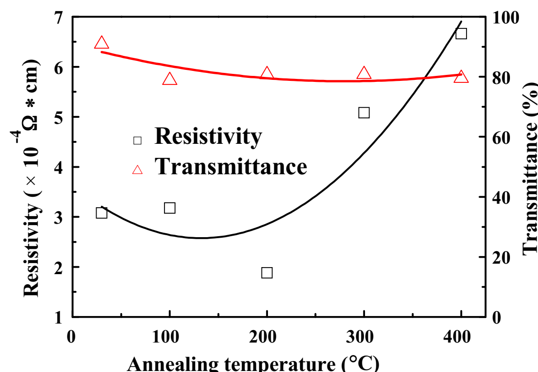

Fig. 4. Resistivity and optical transmittance of ZITO electrode post-annealed at different temperatures.

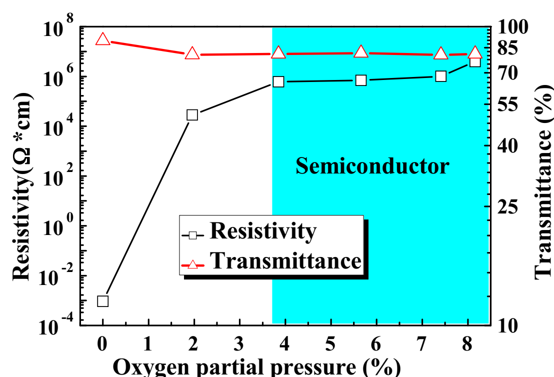

Fig. 5. Resistivity and optical transmittance of ZITO film as functions of O_2 gas concentration $[O_2/(O_2 + Ar)\%]$.

increment of annealing temperature. The main reason is that the crystalline grain size became larger resulted in the amount of trapping states reduced [24]. As annealing temperature was more than 200 °C, the film resistivity rapidly raised which associated with the more zinc acceptor impurities were activated to recombine with the oxygen resulted in reduction of oxygen vacancies [19,25]. The average transmittance in visible region (390–800 nm) of as-deposited film is about 90.9%. When the post-annealing temperatures were raised, the average transmittance in visible region of film slightly decreased which associated with the increment of surface roughness [26]. Briefly, a suitable substrate temperature (100 °C) can promote the film resistivity under the depositing process. However, the resistivity and optical transmittance of ZITO film could not be efficiently improved by a post-annealing.

3.4. Semiconducting ZITO film (Zn atomic concentration ratio of 69% and 89%)

According to the XRD (Fig. 1), the ZITO film with Zn atomic concentration ratio of 69% was an amorphous-like structure that was suitable for the application in thin film transistors (TFTs). To achieve the semiconductor characteristic, the ZITO film with Zn atomic concentration ratio of 69% was selected to adjust the resistivity under the different oxygen partial pressures. Fig. 5 shows the resistivity and optical transmittance of ZITO films under the different oxygen gas concentrations. The resistivity of ZITO films increased with increasing the oxygen gas pressure (0–8%) which revealing the more oxygen interstitials existed in lattice resulted in the amount of electron-trapping centers increased [27]. As the oxygen gas pressure was more than 3.85%, the ZITO films possessed a semiconductor characteristic ($>6.05 \times 10^5\,\Omega\,$cm) that could be applied in TFT devices [28]. In addition, the average transmittance in visible region of all films was about 81% which indicated that the influence of oxygen gas concentration on optical transmittance of ZITO films was not obvious during the depositing processes.

To investigate the luminescence properties of the semiconducting films, the ZITO films under the different oxygen partial pressures (0%, 3.85% and 8.16%) were measured by photoluminescence (PL) at room temperature (Fig. 6(a)). The PL characteristics of present ZITO films presented three distinct emissions in a violet luminescence at 2.95 eV, three green luminescence peaks at 2.41 eV, 2.31 eV and 2.28 eV and two red luminescence peaks at 1.79 eV and 1.75 eV. The violet luminescence can be attributed to the interface traps present at the depletion region near the grain boundaries [29]. The green luminescence originated from the recombination of the holes with the single ionized charge of oxygen-vacancy (V_0^+) [30,31]. The red luminescence was related to the oxygen-vacancy (V_0) or zinc interstitial (Zn_i) [32,33]. Com-

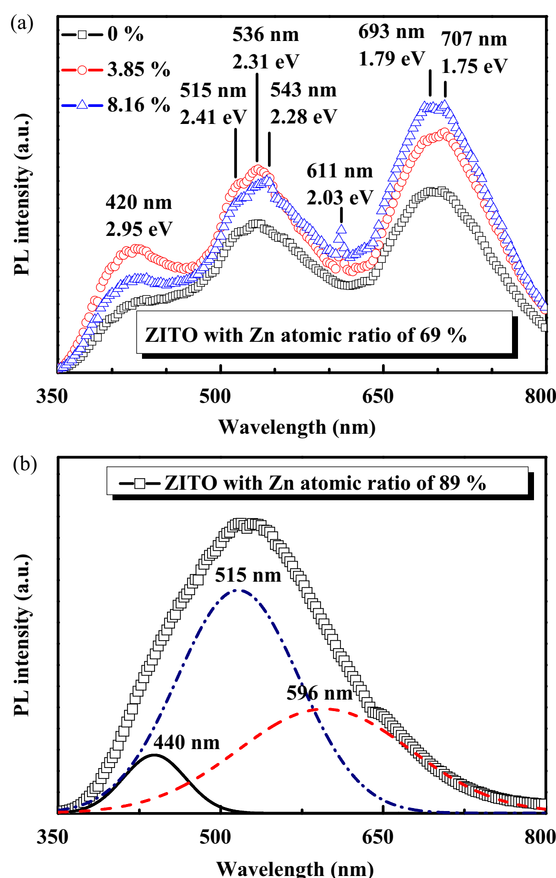

Fig. 6. (a) PL spectrum with different O_2 gas contents for ZITO film with Zn atomic concentration ratio of 69%. (b) PL spectrum of ZITO film with Zn atomic concentration ratio of 89%.

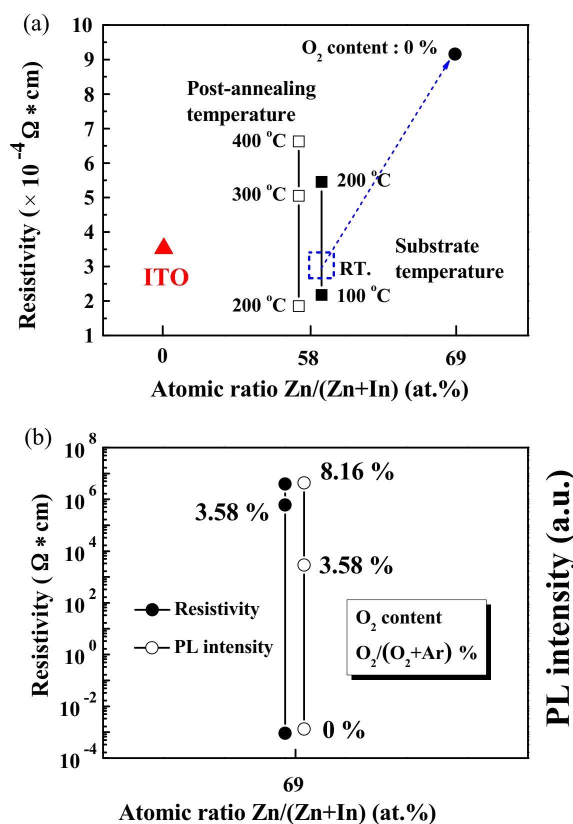

Fig. 7. (a) Variations in resistivity for ZITO (Zn atomic concentration of 58% and 69%) and ITO films at different substrate and post-annealing temperatures. (b) Variations in resistivity and PL intensity for ZITO (Zn atomic concentration of 69%) film at different O_2 gas concentrations.

paring to the ZnO film [5], the violet emission position of present ZITO film exhibited a red-shift from 3.18 eV to 2.95 eV which indicated that the doped ITO resulted in the increment of nonradiative recombination [34]. Notably, when the oxygen gas was injected, the ZITO films presented an orange luminescence peak at 2.03 eV that may be associated with the single ionized oxygen interstitial (O_i^-) [35]. Notably, the intensity of luminescence increased with increasing the oxygen gas content. The main reason is that more defects (singly ionized oxygen and zinc interstitial) were generated during the deposited process. These defects were acted as donor–acceptor pair and further enhanced the luminescence intensity [36].

In addition, the ZITO film with Zn atomic concentration ratio of 89% had a good crystallization and lower cost (the lowest ITO concentration) that may be as a candidate for the active layer of photodetectors. Therefore, PL was used to check its optical quality. Fig. 6(b) shows the PL spectrum (at room temperature) of ZITO film with Zn atomic concentration ratio of 89%. In this spectrum, the film exhibited a broad emission band (violet-yellow emission) which resulted from the deep level or trap state emission [37]. This broad emission can be divided into three emission bands at violet emission of 440 nm (2.82 eV), green emission of 550 nm (2.41 eV) and yellow emission of 596 nm (2.08 eV), respectively. This violet emission was mainly attributed to the radiative recombination related to the interface traps between the grain boundaries [38]. Also, the existence of oxygen vacancies and indium–oxygen vacancy centers probably resulted in the generation of this violet emission [39]. These visible emissions of 550 nm and 596 nm were corresponding to the deep-level emission that originated from the oxygen vacancies in ZITO films and radiative recombination of electron form shallow donors with trapped holes, respectively [40]. According to above results, the ZITO film has good potential to apply in different optoelectronic devices by adjusting the content of ITO phase and oxygen gas.

Notably, the ZITO film with Zn atomic concentration of 58% had a low resistivity ($3.08 \times 10^{-4}\,\Omega\,cm$) that can be as a candidate for TCO material. Under a suitable thermal treatment (substrate temperature of 100 °C or post-annealing temperature of 200 °C), the conductivity of ZITO film had improved (Fig. 7(a)). Judging from the above, the resistivity of ZITO film not only was raised, but also possessed an amorphous phase when the Zn atomic concentration increased to 69%. With increasing the oxygen gas to 3.58%, the ZITO film character was varied from conductor ($9.19 \times 10^{-4}\,\Omega\,cm$) to semiconductor ($3.92 \times 10^{6}\,\Omega\,cm$) (Fig. 7(b)). In addition, higher oxygen gas content could enhance the luminescent property of ZITO films. It is clear that the ZITO film possessed different functions via thermal treatments that could apply in various optoelectronic devices.

4. Conclusions

The ZITO film with Zn atomic concentration ratio of 58% not only had good electrical properties ($\rho \sim 3.08 \times 10^{-4}\,\Omega\,cm$, $\mu \sim 13.9\,cm^2/V\,s$), but also possessed an excellent transmittance in visible region (≥90%). Under the substrate temperature of 100 °C, the film resistivity could be reduced, while the post-annealing could not effectively improve the performance of films.

ITO content decreased (Zn atomic concentration ratio of 69%), the amorphous structure of ZITO film formed. Increased the oxygen gas content (≥3.85%), the active layer of TFTs was obtained and its photoluminescence presented three distinct emissions in violet, green and red region, respectively. In addition, the ZITO film with Zn

atomic concentration ratio of 89% not only had a good crystallization, but also possessed a potential application in photodetectors or gas sensors.

Acknowledgements

The authors are grateful to National Cheng Kung University, the Center for Micro/Nano Science and Technology (D99-2700) and NSC 99-2221-E-006-132 and NSC 99-2622-E-033-CC3 for the financial support.

References

[1] J.K. Kim, J.M. Lee, J.W. Lim, J.H. Kim, S.J. Yun, Jpn. J. Appl. Phys. 49 (2010) 04DP09.
[2] S.H. Lee, S.H. Han, H.S. Jung, H. Shin, J. Lee, J.H. Noh, S. Lee, I.S. Cho, J.K. Lee, J. Kim, H. Shin, J. Phys. Chem. C 114 (2010) 7185–7189.
[3] N.C. Su, S.J. Wang, C.C. Hung, Y.H. Chen, H.Y. Huang, C.K. Chiang, C.H. Wu, A. Chin, Jpn. J. Appl. Phys. 49 (2010) 04DA12.
[4] H.C. Chen, M.J. Chen, M.K. Wu, W.C. Li, H.L. Tsai, J.R. Yang, H. Kuan, M. Shiojiri, IEEE J. Quant. Electron. 46 (2) (2010) 265–271.
[5] K. Jang, H. Park, S. Jung, N.V. Duy, Y. Kim, J. Cho, H. Choi, T. Kwon, W. Lee, D. Gong, S. Park, J. Yi, D. Kim, H. Kim, Thin Solid Films 518 (2010) 2808–2811.
[6] L.W. Ji, C.Z. Wu, C.M. Lin, T.H. Meen, K.T. Lam, S.M. Peng, S.J. Young, C.H. Liu, Jpn. J. Appl. Phys. 49 (2010) 052201.
[7] T. Minami, Thin Solid Films 516 (2008) 1314–1321.
[8] G.S. Heo, Y. Matsuymoto, I.G. Gim, J.W. Park, K.Y. Kim, T.W. Kim, Solid State Commun. 148 (2009) 1731–1734.
[9] G.S. Heo, Y. Matsumoto, I.G. Gim, H.K. Lee, J.W. Park, T.W. Kim, Solid State Commun. 150 (2010) 223–226.
[10] M.K. Ryu, S. Yang, S.H.K. Park, C.S. Hwang, J.K. Jeong, Appl. Phys. Lett. 95 (2009) 072104.
[11] D.H. Lee, S.Y. Han, G.S. Herman, C.H. Chang, J. Mater. Chem. 19 (2009) 3135–3137.
[12] A.E. Solovjeva, V.A. Zhdanov, Inorg. Mater. 21 (1985) 957–960.
[13] K. Tominaga, T. Takao, A. Fukushima, T. Moriga, I. Nakabayashi, Vacuum 66 (2002) 505–509.
[14] D.S. Liu, C.H. Lin, F.C. Tsai, C.C. Wu, J. Vac. Sci. Technol. A 24 (3) (2006) 694–699.
[15] D.S. Liu, C.C. Wu, C.T. Lee, Jpn. J. Appl. Phys. 44 (7) (2005) 5119–5121.
[16] D.S. Liu, C.H. Lin, B.W. Huang, C.C. Wu, Jpn. J. Appl. Phys. 45 (4B) (2006) 3526–3530.
[17] S.W. Shin, K.U. Sim, J.H. Moon, J.H. Kim, Curr. Appl. Phys. 10 (2010) S274–S277.
[18] T. Prasada Rao, M.C. Santhosh Kumar, A. Safarulla, V. Ganesan, S.R. Barman, C. Sanjeeviraja, Physica B 405 (2010) 2226–2231.
[19] D.S. Liu, C.S. Sheu, C.T. Lee, C.H. Lin, Thin Solid Films 516 (2008) 3196–3203.
[20] Y.H. Kim, K.S. Lee, T.S. Lee, B. Chenog, T.-Y. Seong, W.M. Kim, Appl. Surf. Sci. 255 (2009) 7251–7256.
[21] J.S. Hong, S.M. Kim, S.J. Park, H.W. Choi, K.H. Kim, Mol. Cryst. Liq. Cryst. 520 (2010) 19–27.
[22] T. Koida, H. Fujiwara, M. Kondo, Sol. Energy Mater. Sol. Cells 93 (2009) 851–854.
[23] H.J. Cho, S.U. Lee, B. Hong, Y.D. Shin, J.Y. Ju, H.D. Kim, M. Park, W.S. Choi, Thin Solid Films 518 (2010) 2941–2944.
[24] J.K. Sheu, K.W. Shu, M.L. Lee, C.J. Tun, G.C. Chi, J. Electrochem. Soc. 154 (6) (2007) H521–H524.
[25] G. Gonçalves, E. Elangovan, P. Barquinha, L. Pereira, R. Martins, E. Fortunato, Thin Solid films 515 (2007) 8562–8566.
[26] K.J. Chen, F.Y. Hung, S.J. Chang, S.J. Young, Z.S. Hu, S.P. Chang, J. Sol–Gel Sci. Technol. 54 (2010) 347–354.
[27] K.C. Liu, J.R. Tsai, C.S. Li, P.H. Chien, J.N. Chen, W.S. Feng, Jpn. J. Appl. Phys. 49 (2010) 04DF21.
[28] K.J. Saji, M.K. Jayaraj, K. Nomura, T. Kamiya, H. Hosono, J. Electrochem. Soc. 155 (6) (2008) H390–H395.
[29] K.H. Lee, N.I. Cho, E.J. Yun, H.G. Nam, Appl. Surf. Sci. 256 (2010) 4241–4245.
[30] C.W. Na, S.Y. Bae, J. Park, J. Phys. Chem. B 109 (2005) 12785–12790.
[31] D.K. Bhat, Nanoscale Res. Lett. 3 (2008) 31–35.
[32] M.A. Reshchikov, H. Morkoc, B. Nemeth, J. Nause, J. Xie, B. Hertog, A. Osinsky, Physica B 358 (2007) 401–402.
[33] D.H. Kong, W.C. Choi, Y.S. Shin, J.H. Park, T.G. Kim, J. Korean Phys. Soc. 48 (6) (2006) 1214–1217.
[34] K.J. Chen, F.Y. Hung, S.J. Chang, J. Nanosci. Nanotechnol. 8 (2008) 1–5.
[35] B. Yao, L.X. Guan, G.Z. Xing, Z.Z. Zhang, B.H. Li, Z.P. Wei, X.H. Wang, C.X. Cong, Y.P. Xie, Y.M. Lu, D.Z. Shen, J. Lumin. 122–123 (2007) 191–194.
[36] B. Guo, Z.R. Qiu, K.S. Wong, Appl. Phys. Lett. 82 (14) (2003) 2290–2292.
[37] S.T. Jean, Y.C. Her, Cryst. Growth Des. 10 (5) (2010) 2014–2110.
[38] D.H. Fan, Z.Y. Ning, M.F. Jiang, Appl. Surf. Sci. 245 (2005) 414–419.
[39] S. Kaleemulla, A. Sivasankar Reddy, S. Uthanna, P. Sreedhara Reddy, J. Alloy. Compd. 479 (2009) 589–593.
[40] K.J. Chen, F.Y. Hung, Y.T. Chen, S.J. Chang, Z.S. Hu, Mater. Trans. 51 (2010) 1340–1345.